Advances in Radiation Oncology (2025) **10**, 101713

advances in radiation oncology

www.advancesradonc.org

Scientific Article

Integrating Radiosensitivity Index and Radiation Resistance Related Index Improves Prostate Cancer Outcome Prediction

Qi-Qiao Wu, MD,[a,b] Zhao-Sheng Yin, MD,[c,1] Yi Zhang, MD,[d,1] Yu-Fu Lin, MD,[a,e] Jun-Rong Jiang, BS,[d] Ruo-Yan Zheng, BS,[d] Tao Jiang, MD,[f] Dong-Xu Lin, MD,[g] Peng Lai, MD,[h] Fan Chao, PhD,[h] Xin-Yue Wang, MD,[i] Bu-Fu Tang, PhD,[f] Shi-Suo Du, PhD,[f] Jing Sun, MD,[f,*] Ping Yang, MD,[a,e,f,*] and Zhao-Chong Zeng, PhD[f,*]

[a]Clinical Research Center for Precision Medicine of Abdominal Tumor of Fujian Province, China; [b]Department of Radiation Oncology, Fudan University Zhongshan Hospital (Xiamen Branch), China; [c]Heavy Ion Center, Wuwei Cancer Hospital, Wuwei, Gansu, China; [d]Institute of Respiratory Diseases, Xiamen Medical College, Xiamen, Fujian, China; [e]Department of Oncology, Fudan University Zhongshan Hospital (Xiamen Branch), China; [f]Department of Radiation Oncology, Fudan University Zhongshan Hospital, Shanghai, China; [g]Department of Urological Surgery, Jinjiang Municipal Hospital, Quanzhou, Fujian Province, China; [h]Department of Urological Surgery, Fudan University Zhongshan Hospital (Xiamen Branch), Xiamen, China; and [i]Department of Nutrition, Fudan University Zhongshan Hospital (Xiamen Branch), Xiamen, China

Received 21 June 2024; accepted 23 December 2024

Purpose: This study aimed to establish a nomogram combining 31-gene signature (31-GS), radiosensitivity index (RSI), and radiation-resistance-related gene index (RRRI) to predict recurrence in prostate cancer (PCa) patients.

Methods and Materials: Transcriptome data of PCa were obtained from gene expression omnibus and the cancer genome atlas to validate the predictive potential of 3 sets of published biomarkers, namely, 31-GS, RSI, and RRRI. To adjust these markers for the characteristics of PCa, we analyzed 4 PCa-associated radiosensitivity predictive indices based on 31-GS, RSI, and RRRI by the Cox analysis and least absolute shrinkage and selection operator regression analysis. Time-dependent receiver operating characteristic curves, decision curve analyses, integrated discrimination improvement, net reclassification improvement and decision tree model construction were used to compare the radiosensitivity predictive ability of these 4 gene signatures. Key modules and associated functions were identified through a weighted gene co-expression network analysis and gene function enrichment analysis. A nomogram was built to improve the recurrence-prediction capability.

Results: We validated and compared the predictive potential of 2 published predictive indices. Based on the 31-GS, RSI, and RRRI, we analyzed 4 PCa-associated radiosensitivity predictive indices: 14Genes, RSI, RRRI, and 20Genes. Among them, 14Genes showed the most promising predictive performance and discriminative capacity. Genes in the key module defined by the 14Genes model were significantly enriched in radiation therapy-related cell death pathways. The area under receiver operating characteristic curve and decision tree variable importance for 14Genes was the highest in the cancer genome atlas and Gene Expression Omnibus Series (GSE) cohorts.

Sources of support: This work had no specific funding.

Research data are stored in an institutional repository and will be shared upon request to the corresponding author.

[1]Co-first authors.

*Corresponding authors. Jing Sun, MD; Email: sun.jing@zs-hospital.sh.cn, Ping Yang, MD; Email: yang.ping@zs-hospital.sh.cn and Zhao-Chong Zeng, PhD; Email: zeng.zhaochong@zs-hospital.sh.cn.

https://doi.org/10.1016/j.adro.2025.101713

Conclusions: This study successfully established a radiosensitivity-related nomogram, which had excellent performance in predicting recurrence in patients with PCa. For patients who received radiation therapy, the 20Genes and RRRI models can be used to predict recurrence-free survival, whereas 20Genes is more radiation therapy-specific but needs further external validation.

Introduction

Prostate cancer (PCa) is the second most common cancer in men worldwide, with an estimated 288,300 new cases diagnosed and 34,700 deaths in 2023.[1] Radiation therapy is one of the primary treatment options for PCa, and it involves using high-energy radiation to kill cancer cells.[2] However, not all tumors respond equally to radiation therapy, and some patients experience treatment failure despite receiving high doses of radiation. Accordingly, the radiosensitivity index (RSI) has been developed. It is a tool used to predict a patient's response to radiation therapy and is based on the idea that tumors with certain genetic or molecular characteristics may be more sensitive to radiation therapy.[3,4] Therefore, by analyzing these characteristics, predicting which PCa patients will respond well to radiation therapy and have a better recurrence-free survival (RFS) may be possible.[5]

The RSI is a 10-gene model based on the radiation survival at 2Gy (SF2) in 48 human cancer-cell lines.[6] The prediction model is a linear regression algorithm that is validated in esophageal cancer, head and neck cancer, rectal cancer, breast cancer, and endometrial cancer. However, the use of the radiation sensitivity index in clinical practice remains limited, and more research is needed to validate its effectiveness. Nolan et al[7] evaluated the association between RSI and the related genomic-adjusted radiation dose (GARD) model. They found that combining the GARD model with sequencing transcriptomics data may have the potential to provide information for the personalized radiation therapy of PCa patients. A higher dosage guided by the GARD model may have benefited half of the patients in their research. Meanwhile, 31-gene signature (31-GS) has been developed by Kim's group. They analyzed NCI-60 cancer-cell lines (including PCa) for genes whose expression is correlated with that of SF2.[8] The radiation-resistance-related gene index (RRRI) has been developed by Ke et al[9] and validated through the cancer genome atlas (TCGA) and GSE cohort for its good biochemical recurrence predicting ability. Notably, no overlapping genes exist between the 2 radiosensitivity predictive indices. Exactly which genes play an important predictive role in PCa also remains unknown.

In this study, we compared the ability of the above-mentioned gene signatures to predict PCa RFS by using the gene expression omnibus (GEO) and TCGA PCa patient data sets. Four integrating radiosensitivity gene signatures were established based on the 3 signatures and adapted to PCa. Sensitivity and specificity were used to assess the reliability and accuracy of these radiosensitivity biomarkers. A nomogram involving optimum radiosensitivity gene signature was built for PCa prognosis.

Methods and Materials

Acquisition of public data

The transcriptome data of 552 PCa samples were downloaded from the TCGA database (https://portal.gdc.cancer.gov/). We found 426 PCa cases with unabridged data of RFS time after screening. The definition of recurrence encompassed biochemical recurrence (BCR) and distant metastasis, recurrence status, and transcriptome and Gleason score. GSE116918,[10] which included 248 PCa patients having unabridged information (ie, metastasis-free time, metastasis status, BCR-free time, BCR status, and transcriptome and Gleason score) was downloaded from the GEO database (https://www.ncbi.nlm.nih.gov/geo/). For the training cohort, TCGA PCa (552 PCa samples) was used; for the validating cohort, GEO cohort (248 PCa samples) was used. The stage of primary tumor was referred to as T-stage.

Validating the 2 existing radiosensitivity signatures

According to the expression profile of the 2 sets of radiosensitivity-related signature, we categorized the GSE116918 and TCGA data sets into 2 groups. We calculated, RSI as described by Eschrich et al.[6] RRRI[9] was calculated and according to their median risk score, all patients were categorized into high-risk and low-risk score subgroups, accordingly.

Establishing improved radiosensitive models

The RSI and 31-GS are not specific for PCa. They are also based on different cell lines. Accordingly, we used the TCGA data set as a training cohort and the GSE cohort as a validation cohort to identify precise PCa radiosensitivity signatures. The PCa RFS was predicted through Cox and

least absolute shrinkage and selection operator (LASSO) analyses, with the models reformulated as shown below:

N Gene Signature = $\sum$ (Expk * Coek), k = 1, where Expk is the expression value for each gene, Coek is the coefficient of regression models, and n is the number of selected genes. Four radiosensitivity predictive indices, namely, RSI (involving genes in the RSI model), RRRI (involving genes in the RRRI model), 20Genes (involving genes from the RSI and RRRI models), and 14Genes (involving the 14 genes identified via LASSO regression analysis), were identified.

Identification of clinically significant modules

The co-expression module is a collection of genes with high topological overlap similarity. Genes in the same module often have a higher degree of co-expression. The R WGCNA package was used to calculate the correlation coefficients between gene pairs by Pearson's correlation coefficient to construct the gene co-expression matrix.[11] A dendrogram was constructed using hierarchical clustering to calculate the correlation between the module's characteristic genes and the disease phenotype, with the module with the highest correlation coefficient and the smallest *P* value being defined as the disease characteristic.

Gene function enrichment analysis

The R package (clusterProfiler, enrichplot)[12] was used to perform gene ontology (GO) (http://geneontology.org/, accessed on 15 October 2024) and Kyoto Encyclopedia of Genes and Genomes(KEGG) (http://www.genome.jp/kegg/, accessed on 15 October 2024) enrichment analysis of the intersecting genes (DEG, key module genes of the WGCNA screen), with $P < .05$ considered to be a significantly different level for the enrichment result.

Comparing and validating the prognostic indices

Analysis of time-dependent receiver operating characteristic (ROC) curve was performed for comparing the predictive power of our model. To evaluate the model's prognostic potential, we compared the areas under ROC curves (AUCs). The improvement in the model's predictive power on risk-factor addition was estimated using the net reclassification improvement (NRI) and integrated discrimination improvement (IDI). The discriminative ability of the selected risk models for predicting PCa outcomes were evaluated using AUC, NRI, and IDI. Using the R survIDINRI package, the IDI and NRI values of the selected 4 predictors were calculated, with RSI serving as the reference.

Predictive decision tree construction and variable importance visualization

To explore the importance of the 4 different risk score models and clinical factors, T-stage, Gleason score, were extracted from the above analysis and used as input features, and were used along with 4 risks core models to construct the decision tree model using R package, rpart. The variable importance of the decision tree model is analyzed and visualized to understand the impact of different features. The most important feature (the one with the highest importance value) is identified using the which. maximum function. A bar plot is generated to visualize the importance of each variable.

Analysis of the subgroups of selected gene signatures

The PCa is characterized by diverse histologic types, so the correlation of the 4 models with histologic/pathologic features was further explored. One-way ANOVA was used to test TCGA PCa cases, and results of subgroup analysis are shown in violin plots. We performed subgroup KM analysis to determine the discriminability of each radiosensitivity predictor in the radiation therapy (RT) and non-RT groups, and to identify patients who can benefit specifically from RT. The findings of subgroup analysis were analyzed using KM survival plots.

Results

Validation of the predictive capacity for RSI and RRRI signatures

First, we validated the predictive capacity of the RRRI and RSI in the TCGA cohort and GSE116918. According to Eschrich et al,[6] patients in the lower RSI quartile are considered to be in the radiosensitive group, and the rest are in the radio-resistant group. No survival difference was observed between the radiosensitive and radio-resistant groups (Fig. 1F, J, N). Then, the RRRI-defined low-risk group was found to exhibit better survival relative to the high-risk one (Fig. 1G) in the TCGA cohort. In the GSE cohort, no survival difference was observed between the low-risk and high-risk groups (Figs. 2G and 4O).

Integrating radiosensitive genes and constructing the new risk model

Separately, the RRRI and RSI cannot robustly predict RFS in training and validating groups. Considering that 31-GS and RSI gene signatures were developed from

various cell lines and are not PCa specific, we rebuilt the gene signatures based on PCa patients. First, the 50 genes were analyzed by univariate Cox regression. Results showed that not all genes were prognostic factors of PCa, as shown in Fig. 2I. (PTPRCAP was ruled out because of its absent expression in the TCGA cohort).

Correlation analysis further revealed a high correlation between some of the genes (Fig. 4C), thereby highlighting the difficulty of identifying significant genes through traditional statistical methods. Shrinking the number of genes was necessary, so we used LASSO regression analysis to identify important predictive genes (Fig. 4A). To obtain a more accurate prognostic model, we defined λ as the lambda.min (Fig. 4B). A total of 14 corresponding gene numbers were found to be involved, and the 14Genes were calculated as follows:

$$\begin{aligned}\text{Risk score} = {} & (0.00456664 \times \text{ABL1}) \\ & - (0.5180618 \times \text{HCG4}) \\ & + (0.33482162 \times \text{ZNF695}) \\ & - (0.0055657 \times \text{SCNN1A}) \\ & - (0.0011904 \times \text{TSPAN1}) \\ & + (0.03135555 \times \text{IRF7}) \\ & + (0.00501407 \times \text{COMP}) \\ & - (0.0026034 \times \text{CAPNS1}) \\ & + (0.01273938 \times \text{HCLS1}) \\ & + (0.00117237 \times \text{HTRA1}) \\ & + (0.0319295 \times \text{ITGB5}) \\ & + (0.08145763 \times \text{PIR}) \\ & + (0.00460972 \times \text{PKM}) \\ & - (0.0085186 \times \text{PYGB}).\end{aligned}$$

All patients were categorized into high-risk and low-risk score subgroups based on the median risk score.

Weighted co-expression network construction and identification of key modules

Twenty-one modules were identified based on average hierarchical clustering and dynamic tree clipping (Fig. 4E). The Tan module was highly related to the 14Gene defined risk group; thus, this module was selected as radiosensitivity-related gene signature important module for further analysis (Fig. 4F).

Enrichment analysis of KEGG and GO

The KEGG signaling pathway and GO analyses showed that the signature genes were most enriched in pathways related to the cell cycle, DNA replication, base excision repair, and mismatch repair (Fig. 4H), and in chromosome segregation, chromosomal region, and catalytic activity on DNA (Fig. 4I). These findings align with mechanisms involved in radiation therapy-induced DNA damage.

Validation and comparison of prognostic indices

We used TCGA as the training group and compared the time-dependent ROCs to determine the prognostic potential of these gene signature scores. The time-dependent ROC curves for 1-year, 3-year, and 5-year survival in the TCGA cohort are shown in Figs. 1A−3D. At all-time points, the 14Genes score had the highest AUC, followed by RRRI and 20Genes. To compare the predictive accuracy of the selected 4 sets of markers, we performed IDI and NRI analyses. Given that RSI's AUC was the lowest, RSI was chosen as a referent marker. The other 3 predictors exhibited significant capacity to predict survival ($P \leq .05$). Consistent with the ROC curve results, 14Genes had the highest IDI and NRI value at all time points, followed by RRRI, then 20Genes (Figs.5 A-C). On addition, we conducted a survival decision tree analysis using risk scores alongside clinical features, such as Gleason score and T-stage, to identify risk subgroups (Figs. 5G-I]). This analysis showed that the 14Gene model had the highest variable importance in the TCGA and GSE (Met) cohorts and ranked second in the GSE (BCR) cohort (Figs. 5J-L). The KM curve analyses were performed to display the prognostic value of these prognostic indices. The results showed that patients in the high-risk prognostic index group tended to have shorter RFS (Figs. 1E-H).

Similar results were obtained from external validation (Fig. 2). Time-dependent ROC curves for 1-, 3-, and 5-year metastasis-free survival and biochemical RFS in the GSE cohort are shown in Figs. 2A-D and Figs. 2I-L. 14Genes had the highest AUC for 1-year, 3-year, and 5-year metastasis-free survival and biochemical RFS, followed by RSI for 1-year, 3-year metastasis-free survival and biochemical RFS, RRRI for the 5-year metastasis-free survival and 5-year biochemical RFS; KM curve analyses also showed that high-risk groups evaluated by all the prognostic indices appeared to have a worse prognosis than those with the low-level counterparts (Figs. 2E-H and 2M-P).

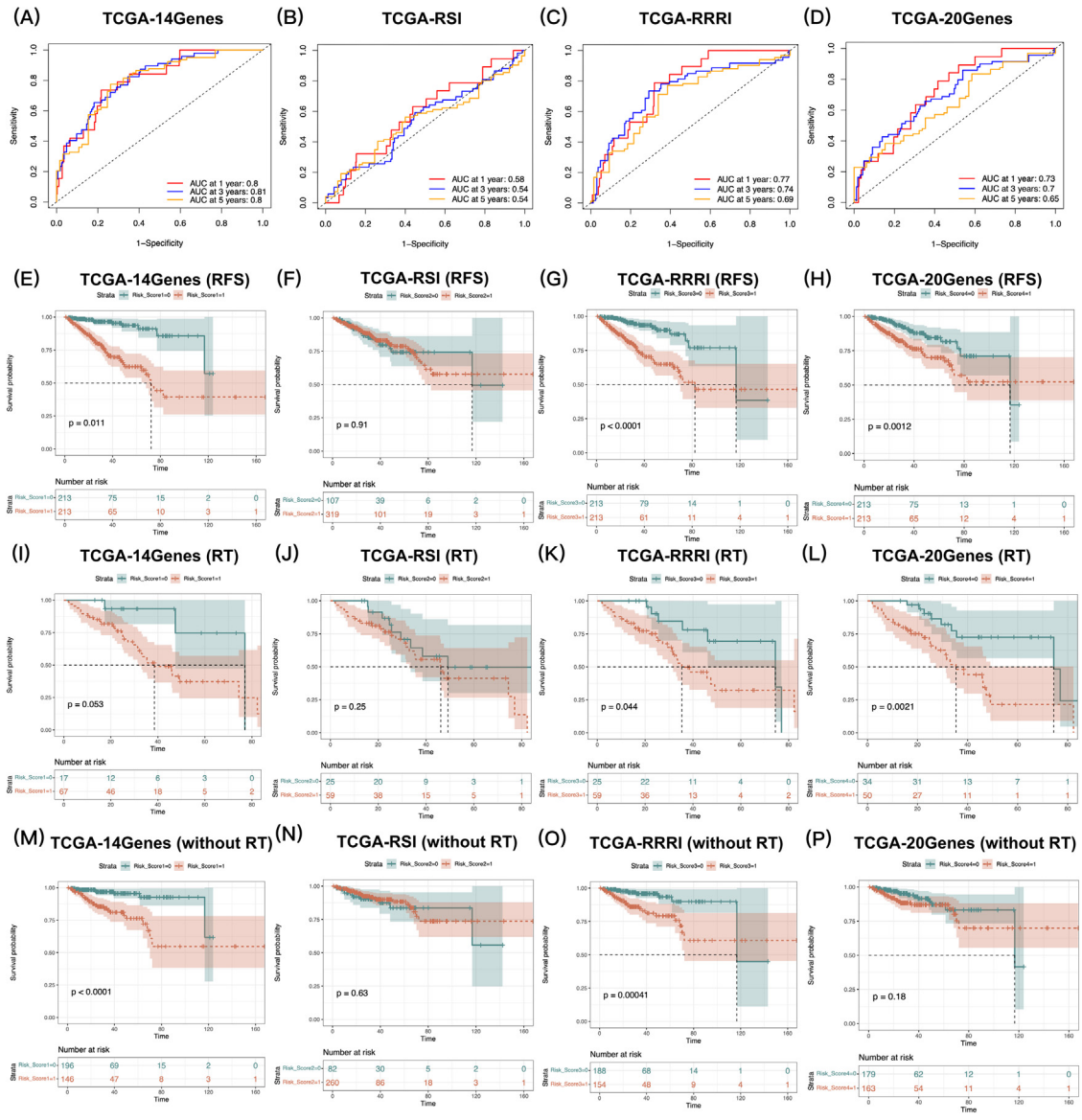

Figure 1 (A-D) Time-ROC curves for 1-year, 3-year, and 5-year RFS prediction between different risk models in TCGA (training cohort); (E-H) KM analysis of different risk models for their RFS; (I-L) KM analysis of different risk models for their RFS in patient group who received RT; and (M-P) KM analysis of different risk models for their RFS in patient group who did not received RT. *Abbreviations*: ROC = receiver operating characteristic; RFS = recurrence-free survival; TCGA = the cancer genome atlas; RT = radiation therapy.

Construction of a nomogram for predicting prostate cancer recurrence-free survival

As 14Genes exhibited significant superiority in survival prediction in both cohorts, we used it as a variable in nomogram construction. After Cox regression analysis of the TCGA data set (training cohort), T stages, Gleason score, and risk scores remained (Fig. 6B). A nomogram was then constructed based on the selected variables to predict the 1-year, 3-year, and 5-year RFS rates (Fig. 6A). We then validated the nomogram externally through the C-index (0.75), calibration curve, and decision curve analyses of the validation cohort. Nomogram calibration plots showed that the predicted 1-year, 3-year, and 5-year survival probabilities in the validated cohort were almost identical to actual observations (Figs. 6C-E). Decision curve analysis showed that the net benefits indicated by the nomogram for 14Genes were higher than those from RRRI, RSI, or 20Genes in TCGA and GEO (BCR) (Figs. 5D-F). Conversely, RSI exhibited the best net benefit for metastasis-free survival (Fig. 5E).

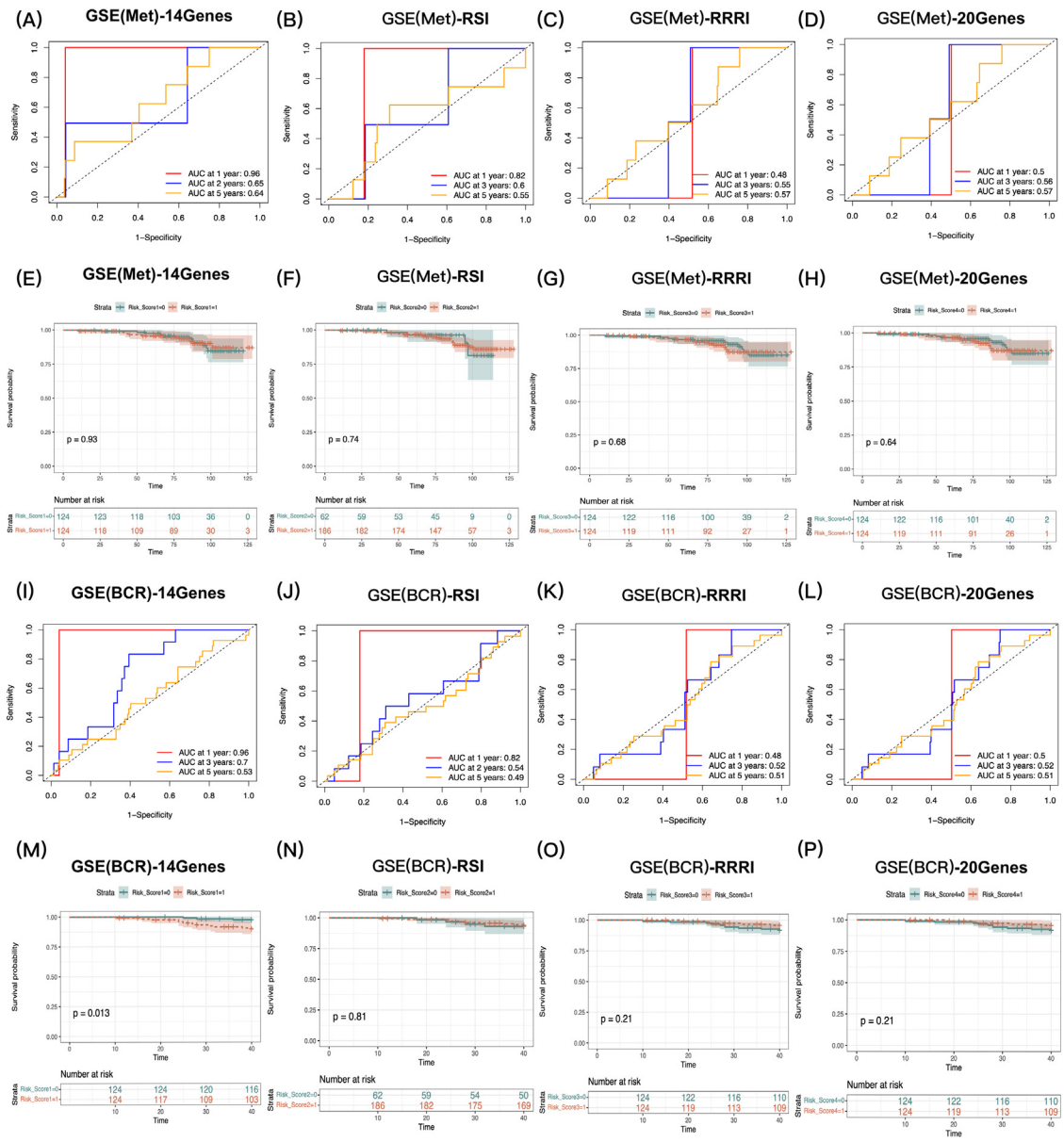

Figure 2 (A-D) Time-ROC curves for 1-year, 3-year, and 5-year metastasis-free survival prediction between different risk models in GSE116918 (validating cohort); (E-H) KM analysis of different risk models for their metastasis-free survival; (I-L) Time-ROC curves for 1-year, 3-year, and 5-year biochemical recurrence-free survival prediction between different risk models in GSE116918 (validating cohort); (M-P) KM analysis of different risk models for their biochemical recurrence-free survival.

Comparing the discrimination capability of selected radiosensitivity predictors

In the TCGA cohort, we built 14Genes and investigated the association of 14Genes score with pathologic characteristics. In the training cohort, the 14Genes score increased with increased T-stage (Fig. 3A). The high-risk group defined by the Gleason score also showed higher 14Genes scores than the low-risk group (Fig. 3B). We tested the discrimination capability of the 4 models by KM analysis of the RT and non-RT groups. Promising radiosensitivity predictive index was expected to distinguish between survival outcomes in the RT population without influencing the outcome of the non-RT patients. We found that RRRI and 20Genes revealed prognostic potential on outcome in the RT groups (Figs. 1K-L), whereas using 20Genes in the non-RT group did not reveal its significance.

Discussion

In recent years, more studies are focusing on the radiosensitivity gene signature of various cancers and their

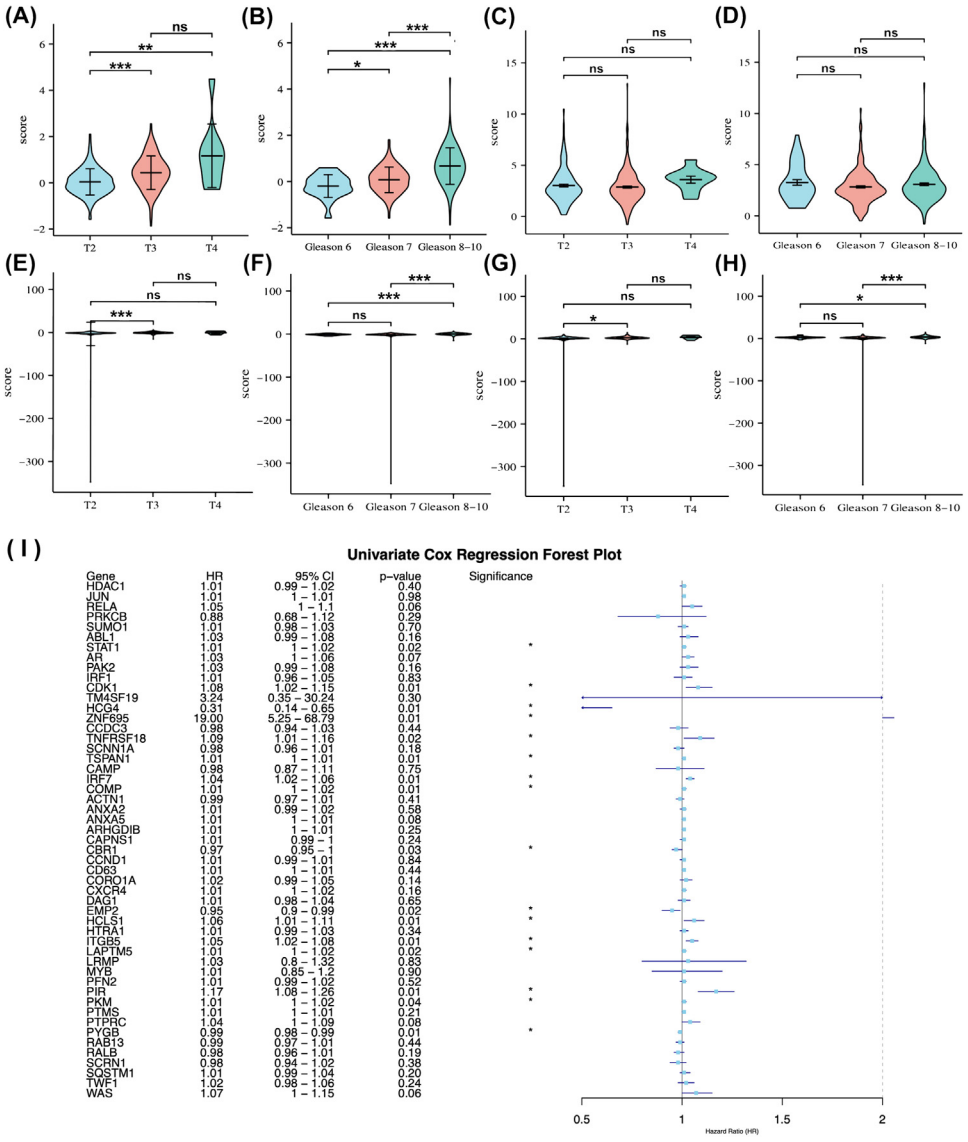

Figure 3 (A) 14Genes expression between difference Stages; (B) 14Genes expression between difference Gleason Scores; (C) RSI expression between difference Stages; (D) RSI expression between difference Gleason Scores; (E) RRRI expression between difference Stages; (F) RRRI expression between difference Gleason Scores; (G) 20Genes expression between difference Stages; (H) 20Genes expression between difference Gleason Scores (*$P < .05$; **$P < .01$; ***$P < .001$.); (I) Univariate Cox Regression Forrest plot of the 50 genes. (I) Univariate Cox regression of 50 genes. *Abbreviation:* RRRI = radiation-resistance-related gene index.

tumor microenvironments.[13] The results can be useful in predicting survival outcome or in guiding a more personalized treatment plan. A very promising future of these studies is that some patients can receive reduced radiation doses according to their gene expression or even have postsurgical radiation therapy waived. For example, the 21-gene recurrence score[14] in breast cancer has been shown to correlate closely with Ki-67 expression levels,[15] facilitating the identification of low-risk recurrence score groups. This enables the selection of patients who may safely omit their postsurgical radiation therapy.[16] Furthermore, the recurrence score classification can also be referred for decision-making on adjuvant chemotherapy in the current National Comprehensive Cancer Network treatment guidelines.[14] Similarly, our study demonstrated that the 14-gene signature was the only model that exhibited significant variation across different Gleason score groups (Fig. 3B). This finding has substantial clinical implications, particularly given the large proportion of elderly prostate cancer patients with comorbidities that may preclude RT. Genetic profiling from biopsy tissue in the definitive treatment setting could identify patients who may either avoid RT or receive lower doses that would minimize adverse effects on quality of life. In addition, the model may help stratify high-risk patients, for whom dose escalation could improve recurrence

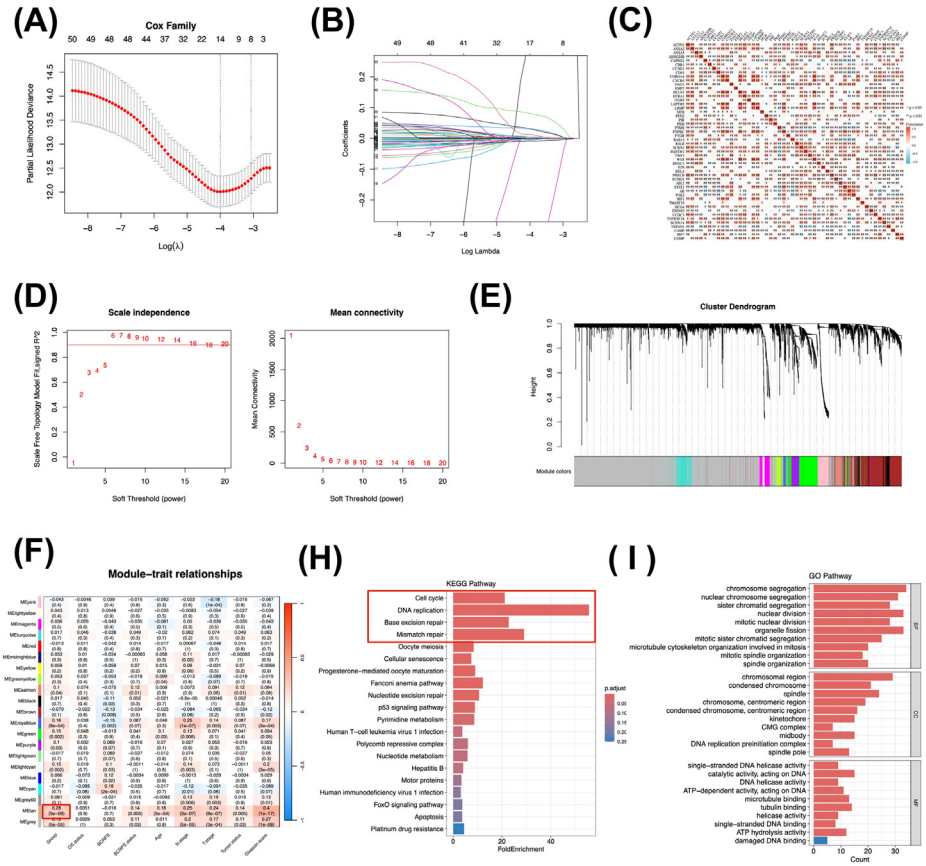

Figure 4 (A) Construction of lasso-Cox model and 14Genes (B) Log (lambda) value of the 50 genes in LASSO regression analysis; (C) correlation heatmap between 31-GS, RSI and RRRI genes; (D) Soft threshold (power = 10) and scale-free topology fit index ($R^2 = 0.90$) (E) Gene hierarchy tree-clustering diagram. The graph indicates different genes horizontally and the uncorrelatedness between genes vertically, the lower the branch, the less uncorrelated the genes within the branch, ie, the stronger the correlation; (F) Heatmap showing the relations between the module and the 14Genes defined high- and low- risk group, the Tan module was highly related to 14Gene defined risk group (as shown in the red border); (H) Functional annotation of the KEGG signaling pathway of signature genes; and (I) GO functional annotation of signature genes. For all enriched GO and KEGG terms, $P < .05$.

control. The 14-gene signature can add to established prognostic factors, such as Gleason score, T-stage, PSA, and the 22-gene genomic classifier (eg, Decipher),[17,18] to identify patients who are suitable candidates for active surveillance.

Several of these 14 genes have been proven to participate in developing various cancers. Larkin et al,[19] constructed a model using ANPEP (Alanyl Aminopeptidase, Membrane) and ABL1 (C-Abl Oncogene 1, Non-Receptor Tyrosine Kinase) as predictors of Gleason grouping and INMT (Indolethylamine N-Methyltransferase) as a predictor of PCa recurrence. In our study, we further indicated the application of ABL1 as a radiosensitivity-related survival predictor. Zhang et al[20] demonstrated that ZNF695 with Gleason score can be used for the diagnosis and prognosis prediction of PCa. Takahashi T et al[21] believed that ZNF695 methylation was significantly correlated with definitive chemoradiotherapy and can be used to predict the response to definitive chemoradiotherapy. Cai et al[22] reported that SCNN1A expression can accelerate ovarian cancer-cell proliferation and migration. Wu et al[23] showed that TSPAN1 can mediate the PI3K/AKT pathway to suppress the growth and motility of breast cancer. Munkley J et al[24] also reported that TSPAN1 can be considered as an androgen-driven contributor to cell survival and motility in PCa. Englund E et al[25] demonstrated that COMP (Cartilage Oligomeric Matrix Protein) can promote PCa progression by acting in an antiapoptosis fashion by interfering with the Ca^{2+} homeostasis of cancer cells. The CAPNS1 has been studied as a hyperactivated molecule in PCa tumor cells and associated with chemotherapy sensitization. However, its role in PCa patients' biologic behavior and radiosensitivity remains unknown.[26] In high-grade primary PCa, tumor with high plasma HCLS1 content is reportedly associated with increased predicted response to immunotherapy and

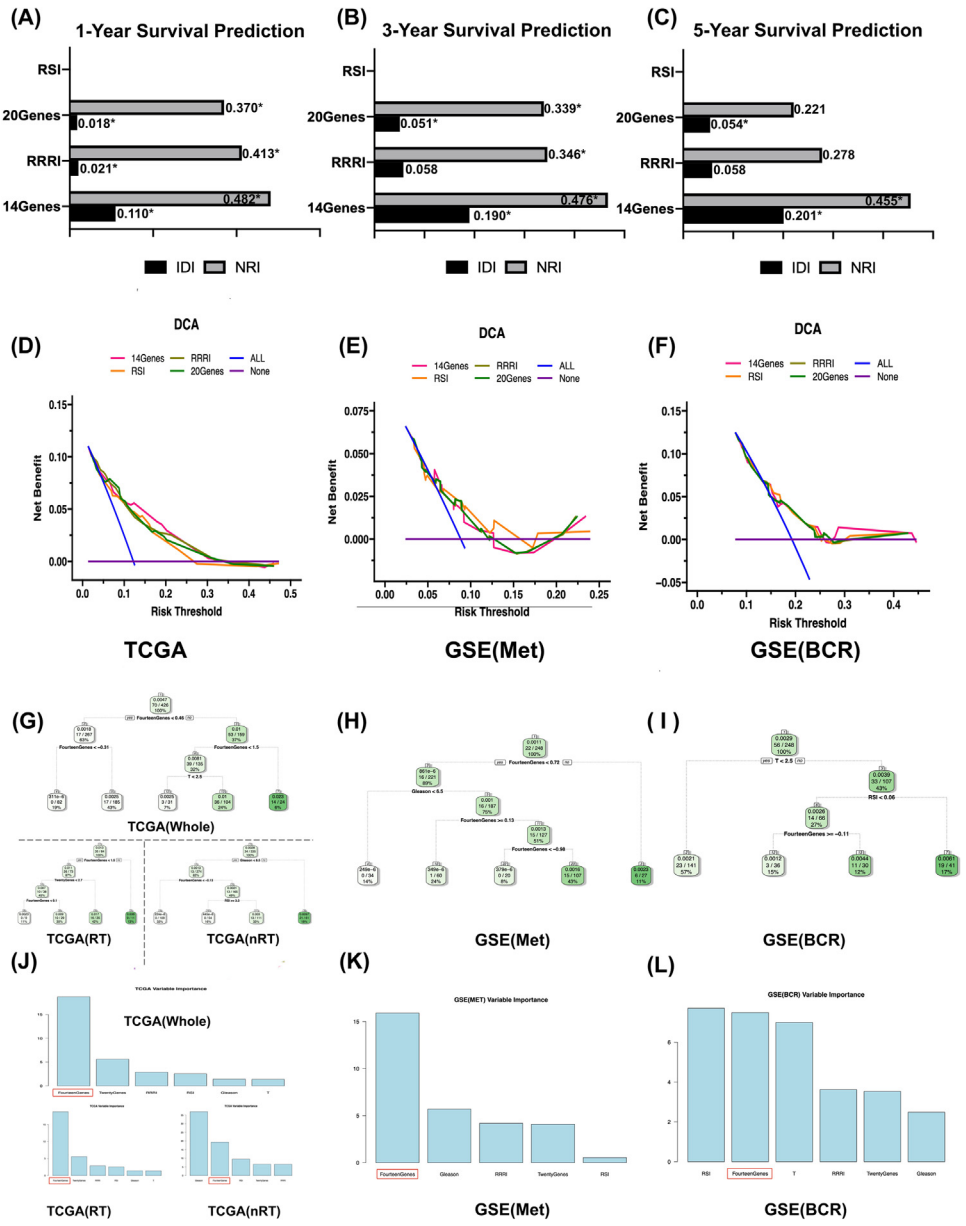

Figure 5 (A-C) Integrated discrimination improvement (IDI) and Net reclassification improvement (NRI) were calculated to compare the predictive accuracy of the 4 selected markers for 1-year, 3-year, and 5- year (* $P < .05$); (D-F) Decision curve analysis from the training and validating group for recurrence-free survival. (G-I) Decision Tree construction for TCGA and its subgroup, GSE(Met), GSE(BCR); (J-L) The variable importance bar plot shows that the 14Gene model ranked highest in the TCGA and GSE (Met) cohorts and second in the GSE (BCR) cohort (highlighted in the red border).

decreased response to androgen-deprivation therapy.[27] Our study further indicated that it was associated with the RFS of PCa patients. Yang et al[28] found that the inhibition of ITGB5 suppresses PCa by affecting the proliferation, invasion, and migration capabilities of cancer cells. A study[29] revealed that the miR-455-5p/PIR (Pirin) axis contributed to PCa cancer-cell aggressiveness, suggesting that PIR may be a promising diagnostic marker for hormone-sensitive PCa and castration-resistant PCa. A high expression of PKM (Pyruvate Kinase M1/2) is reportedly correlated significantly with shorter PFS (Progression Free Survival) in PCa.[30] A previous study has indicated that PYGB (Glycogen Phosphorylase B) is upregulated in PCa tissues and associated with disease progression, [31] in accordance with our results.

Our study had a few limitations. First, samples were downloaded from the TCGA and GEO databases, and information on the extent of tumor nodal stage and radiation status in the GEO cohort was unavailable. In radiation-status-related analysis, we used TCGA to test if the RT-

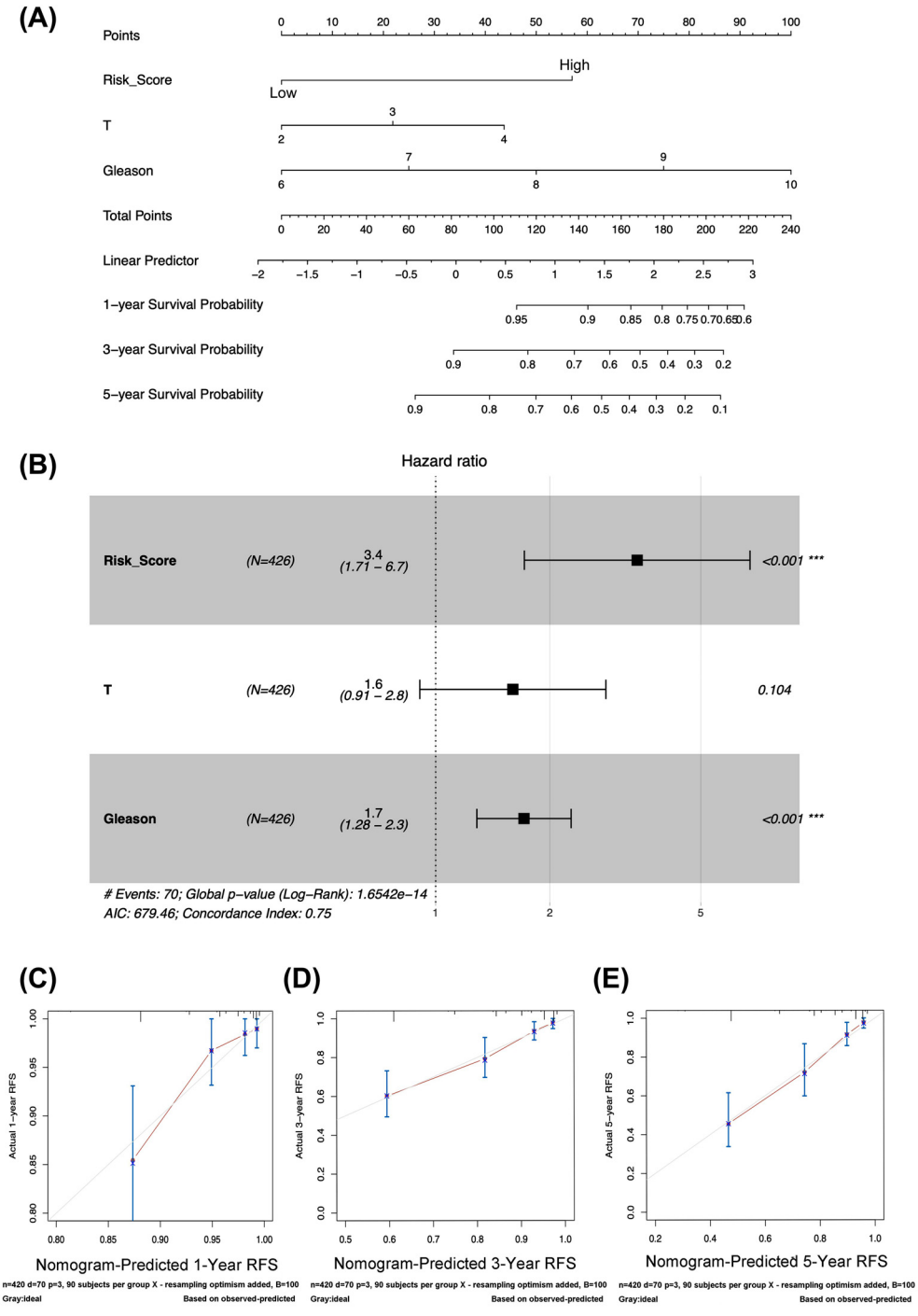

Figure 6 Construction and validation of a Nomogram (A) The nomogram predicting 1-year, 3-year, and 5-year year survival; (B) forest plot of Cox regression model; (C) calibration plots of the nomogram showed that the predicted 1-year, 3-year, and 5-year survival probabilities of the RFS almost identical to the actual observations.

related survival outcome was correlated with the different risk groups defined by 14Genes, RRRI, RSI, and 20Genes. Further analysis with more detailed clinical information is needed. Further prospective research and multicenter clinical trials are needed to validate and refine the model.

Disclosures

The authors declare that they have no known competing financial interests or personal relationships that could have appeared to influence the work reported in this paper.

Acknowledgments

We express our great gratitude to all the people who contributed to this work. Qi-Qiao Wu was responsible for statistical analysis.

Supplementary materials

Supplementary material associated with this article can be found in the online version at doi:10.1016/j.adro.2025.101713.

References

1. Siegel RL, Miller KD, Wagle NS, Jemal A. Cancer statistics, 2023. *CA Cancer J Clin*. 2023;73:17-48.
2. Laughlin BS, Silva AC, Vora SA, et al. Long-term outcomes of prostate intensity-modulated radiation therapy incorporating a simultaneous intra-prostatic MRI-directed boost. *Front Oncol*. 2022;12:921465.
3. Kogionou P, Fortis S, Goulielmaki M, et al. Radiotherapy-related gene signature in prostate cancer. *Cancers*. 2022;14(20):1-15.
4. Ahmed KA, Caudell JJ, El-Haddad G, et al. Radiosensitivity differences between liver metastases based on primary histology suggest implications for clinical outcomes after stereotactic body radiation therapy. *Int J Radiat Oncol Biol Phys*. 2016;95(5):1399-1404.
5. Zhao SG, Chang SL, Spratt DE, et al. Development and validation of a 24-gene predictor of response to postoperative radiotherapy in prostate cancer: a matched, retrospective analysis. *Lancet Oncol*. 2016;17(11):1612-1620.
6. Eschrich S, Zhang H, Zhao H, et al. Systems biology modeling of the radiation sensitivity network: A biomarker discovery platform. *Int J Radiat Oncol Biol Phys*. 2009;75(2):497-505.
7. Nolan B, O'Sullivan B, Golden A. Exploring breast and prostate cancer RNA-seq derived radiosensitivity with the Genomic Adjusted Radiation Dose (GARD) model. *Clin Transl Radiat Oncol*. 2022;36:127-131.
8. Kim HS, Kim SC, Kim SJ, et al. Identification of a radiosensitivity signature using integrative metaanalysis of published microarray data for NCI-60 cancer cells. *BMC Genomics*. 2012;13:348.
9. Bin KZ, You Q, Chen JY, et al. A radiation resistance related index for biochemical recurrence and tumor immune environment in prostate cancer patients. *Comput Biol Med*. 2022;146:105711.
10. Jain S, Lyons CA, Walker SM, et al. Validation of a metastatic assay using biopsies to improve risk stratification in patients with prostate cancer treated with radical radiation therapy. *Ann Oncol*. 2018;29:215-222.
11. Langfelder P, Horvath S. WGCNA: an R package for weighted correlation network analysis. *BMC Bioinformatics*. 2008;9:559.
12. Yu G, Wang L-G, Han Y, He Q-Y. clusterProfiler: an R package for comparing biological themes among gene clusters. *Omics*. 2012;16:284-287.
13. Grass GD, Alfonso JCL, Welsh E, et al. The radiosensitivity index gene signature identifies distinct tumor immune microenvironment characteristics associated with susceptibility to radiation therapy. *Int J Radiat Oncol Biol Phys*. 2022;113:635-647.
14. Turashvili G, Wen HY. Multigene testing in breast cancer: What have we learned from the 21-gene recurrence score assay? *Breast J*. 2020;26:1199-1207.
15. Lee J, Lee Y-J, Bae SJ, et al. Ki-67, 21-gene recurrence score, endocrine resistance, and survival in patients with breast cancer. *JAMA Netw Open*. 2023;6:e2330961.
16. Xie SJ, Wang RJ, Wu SG, Zhang FX. 21-gene recurrence score in predicting the outcome of postoperative radiotherapy in T1-2N1 luminal breast cancer after breast-conserving surgery. *Breast*. 2024;74:103679.
17. Feng FY, Huang HC, Spratt DE, et al. Validation of a 22-gene genomic classifier in patients with recurrent prostate cancer: An ancillary study of the NRG/RTOG 9601 randomized clinical trial. *JAMA Oncol*. 2021;7:544-552.
18. Spratt DE, Liu VYT, Michalski J, et al. Genomic classifier performance in intermediate-risk prostate cancer: results from NRG oncology/RTOG 0126 randomized phase 3 trial. *Int J Radiat Oncol Biol Phys*. 2023;117:370-377.
19. Larkin SET, Holmes S, Cree IA, et al. Identification of markers of prostate cancer progression using candidate gene expression. *Br J Cancer*. 2012;106:157-165.
20. Zhang L, Li Y, Wang X, et al. Five-gene signature associating with Gleason score serve as novel biomarkers for identifying early recurring events and contributing to early diagnosis for Prostate Adenocarcinoma. *J Cancer*. 2021;12:3626-3647.
21. Takahashi T, Yamahsita S, Matsuda Y, et al. ZNF695 methylation predicts a response of esophageal squamous cell carcinoma to definitive chemoradiotherapy. *J Cancer Res Clin Oncol*. 2015;141:453-463.
22. Cai C, Zhang Y, Peng X. Knocking down sterol regulatory element binding protein 2 (SREBF2) inhibits the serine protease 8 (PRSS8) /sodium channel epithelial 1alpha subunit (SCNN1A) axis to reduce the cell proliferation, migration and epithelial-mesenchymal transformation of ovarian cancer. *Bioengineered*. 2021;12:9390-9400.
23. Wu Y, Chen W, Gong Y, Liu H, Zhang B. Tetraspanin 1 (TSPAN1) promotes growth and transferation of breast cancer cells via mediating PI3K/Akt pathway. *Bioengineered*. 2021;12:10761-10770.
24. Munkley J, McClurg UL, Livermore KE, et al. The cancer-associated cell migration protein TSPAN1 is under control of androgens and its upregulation increases prostate cancer cell migration. *Sci Rep*. 2017;7:5249.
25. Englund E, Canesin G, Papadakos KS, et al. Cartilage oligomeric matrix protein promotes prostate cancer progression by enhancing invasion and disrupting intracellular calcium homeostasis. *Oncotarget*. 2017;8:98298-98311.
26. Jorfi S, Ansa-Addo EA, Kholia S, et al. Inhibition of microvesiculation sensitizes prostate cancer cells to chemotherapy and reduces docetaxel dose required to limit tumor growth in vivo. *Sci Rep*. 2015;5:13006.
27. Weiner AB, Yu CY, Kini M, et al. High intratumoral plasma cells content in primary prostate cancer defines a subset of tumors with potential susceptibility to immune-based treatments. *Prostate Cancer Prostatic Dis*. 2023;26:105-112.
28. Yang Y, Feng Q, Hu K, Cheng F. Using CRISPRa and CRISPRi Technologies to Study the Biological Functions of ITGB5, TIMP1, and TMEM176B in Prostate Cancer Cells. *Front Mol Biosci*. 2021;8:676021.
29. Arai T, Kojima S, Yamada Y, et al. Pirin: a potential novel therapeutic target for castration-resistant prostate cancer regulated by miR-455-5p. *Mol Oncol*. 2019;13:322-337.
30. Zhang L, Wang B, Wang ZS, Guo YL, Shen H. Construction of glycolytic regulator gene signature to predict the prognosis and tumor immune cell infiltration levels for prostate cancer. *Comput Math Methods Med*. 2022;2022:9273559.
31. Wang Z, Han G, Liu Q, Zhang W, Wang J. Silencing of PYGB suppresses growth and promotes the apoptosis of prostate cancer cells via the NFκB/Nrf2 signaling pathway. *Mol Med Rep*. 2018;18(4):3800-3808.